RSC Advances

PAPER

View Article Online
View Journal | View Issue



Cite this: *RSC Adv.*, 2022, **12**, 2026

# Nanozymes with reductase-like activities: antioxidant properties and electrochemical behavior

Nataliya Stasyuk, *[ab] Galina Gayda, [a] Taras Kavetskyy[bc] and Mykhailo Gonchar[ab]

Received 5th November 2021
Accepted 5th January 2022

DOI: 10.1039/d1ra08127f

rsc.li/rsc-advances

Nanozymes (NZs) as stable cost-effective mimics of natural enzymes may be promising catalysts in food and environmental biotechnology, biosensors, alternative energy and medicine. The majority of known NZs are mimetics of oxidoreductases, although there are only limited data regarding mimetics of reductases. In the present research, a number of metal-based NZs were synthesized *via* chemical methods and screened for their antioxidant ability in solution. The most effective reductase-like Zn/Cd/Cu NZ was characterized in detail. Its antioxidant properties in comparison with several food products and Trolox, as well as substrate specificity, size and composition were studied. Zn/Cd/Cu NZ was shown to mimic preferentially selenite reductase. The amperometric sensor was constructed possessing a high sensitivity (1700 A $M^{-1}$ $m^{-2}$) and a broad linear range (16–1000 μM) for selenite ions. The possibility to apply the fabricated sensor for selenite determination in commercial mineral water has been demonstrated.



## Introduction

In recent years, nanomaterials with enzyme-mimetic properties (nanozymes) have attracted considerable attention.[1–3] Nanozymes (NZs) as artificial enzymes (AEs) are promising alternatives to the natural ones.[1–5] AEs have essential advantages over natural enzymes such as low preparation costs, stability, high surface area, self-assembling capability, size and composition-dependent activities, broad possibility for modification, and biocompatibility. They have wide potential practical applications as catalysts in biosensors, fuel-cell technology, environmental biotechnology, and medicine.[5–12] It has been shown that AEs mimic the activity of peroxidases,[5,13–15] oxidases,[5,16] superoxide dismutases,[5,17] and hydrolases,[5,18] although only limited data were reported regarding reductase mimetics.[19–25]

Natural reductases are the enzymes which belong to the E.C. 1 class of oxidoreductases and catalyze reduction reactions. Reductases are dehydrogenases which transfer hydrogen from the substrate to biological acceptors and to dyes.[26,27] Reductases lower the activation energy needed for redox reactions to occur. The substrates of microbial reductases are inorganic compounds, including metal ions, metals, and non-metal and metalloid oxianions, as well as organic compounds, including aldehydes, glutathione, nucleotides, proteins, *etc.*[26–42]

Diverse enzymes of various microorganisms take part in the reduction processes, that possess abilities of the metalloreductase,[28,29] carboxylic acid reductase,[30,31] selenate[32] and selenite reductases,[33–36] hydrogenase,[37] cromate reductase,[38,39] nitrite[40] and nitrate reductases[41] *etc.* However, the problem of identification and classification for many reductases was not solved up to day. For example, so far no gene product or enzyme solely responsible for selenite reduction in aerobic bacteria has been identified *in vivo*.[42]

All known NZs usually utilize oxygen or hydrogen peroxide to produce active oxygen forms to oxidize substrate. There exist limited data on the nanomaterials simulating reductase, since oxygen, rather than other biomolecules, is preferable to be reduced on the surface of nanoparticles.[19,22,43] Therefore, it is a great challenge to develop novel mimetics of reductase to simulate its natural counterparts with diverse functions.

Reduction of different substrates using reductase-like (R-like) NZs as catalysts have so far been reported.[19–25] Cr(VI) may be reduced to Cr(III) *via* catalysis by magnetite-based nanocomposites[25] or by cobalt oxide containing nanocomposite,[24] peroxynitrite – *via* grapheme-hemin hybrid nanosheets,[44] and Cyt *c* – *via* zeolitic imidazolate frameworks encapsulated with polyethylenimine.[19] A number of NZs were reported to catalyze the sodium borohydride-induced 4-nitrophenol reduction to 4-aminophenol, namely silver and gold nanoparticles,[23] platinum nanoparticles,[45] reduced graphene oxide–cobalt oxide-based nanocomposite,[24] iron oxide-loaded alginate-bentonite hydrogel beads[20] and other materials.[21,22]

In this paper, we demonstrate that hybride Zn/Cd/Cu (core/shell) NZ obtained *via* the chemical bath deposition method (further – Zn/Cd/Cu$^{bd}$) possesses the ability to mimic reductase,

[a]*Institute of Cell Biology, National Academy of Sciences of Ukraine, 79005 Lviv, Ukraine. E-mail: stasuk_natalia@ukr.net; galina.gayda@gmail.com; gonchar@cellbiol.lviv.ua*

[b]*Drohobych Ivan Franko State Pedagogical University, 82100 Drohobych, Ukraine. E-mail: kavetskyy@yahoo.com*

[c]*The John Paul II Catholic University of Lublin, 20-950 Lublin, Poland*

Table 1 R-like activities of the synthesized AEs in solution

| No. | AE | Synthesis method | Specific activity, U $mg^{-1}$ |
|---|---|---|---|
| 1 | $Zn/Cu/Cd^{bd}$ | Chemical bath deposition on plate | 32.7 ± 1.8 |
| 2 | $Ce/Cu^{bd}$ | | 14.3 ± 1.1 |
| 3 | $Pd/Cu^{bd}$ | | 0.27 ± 0.03 |
| 4 | $Cd/Cu^{cr}$ | Chemical reduction | 3.60 ± 0.25 |
| 5 | $Ce/Pd^{cr}$ | | 0.81 ± 0.02 |
| 6 | $Cu/Pt^{cr}$ | | 1.63 ± 0.15 |
| 7 | $Ce^{cr}$ | | 1.50 ± 0.04 |
| 8 | $Pd/Cd^{cr}$ | | 3.24 ± 0.22 |

in particular, coenzyme-dependent selenite reductase. The synthesized selenite R-like NZ has been used for construction of a highly sensitive amperometric biosensor for selenite detection in water. Based on our findings, we envision that $Zn/Cd/Cu^{bd}$ NZ can also be promising for remediation of waste waters by reducing Se(IV) to elemental selenium ($Se^0$) and for isolation of this element in pure form. The detailed study of effective R-like AEs, including $Zn/Cd/Cu^{bd}$ NZ, may be useful in fundamental biological investigations, in particular, for elucidation of mechanisms of their interactions with living cells. R-like AEs may become potential tools in medicine not only for diagnostics and drug delivery, but also be used as pharmaceuticals (mimetics of antioxidant enzymes) in enzyme-therapy of different diseases caused by unbalance of redox processes in organism.[9–12,46–49]

## Results and discussion

### Obtaining and characterization of reductase mimetics

**Synthesis and screening on pseudo-reductase activity.** A number of metal-based composite materials were synthesized using the methods of chemical reduction (cr) and chemical bath deposition (bd) on plate as potential AEs. The synthesized compounds were screened on their ability to reduce $ABTS^+$ [2,2′-azinobis-(3-ethylbenzothiazoline-6-sulfonic acid) diammonium salt cation radical] in solution (Table 1). It was shown that several synthesized AEs, especially $Zn/Cd/Cu^{bd}$ and $Ce/Cu^{bd}$, possessed the significant reductase-like (R-like) activities.

**Morphological properties of the best reductase mimetics.** The shape and size of the synthesized NZs were characterized by SEM. It was demonstrated (the data are not shown) that the sizes of all studied compounds do not satisfy the nanoscale criterion – to be less than 100 nm in all three dimensions. In some cases, they are nanoscale only in one dimension (needle), while in the other ones they exceed this criterion. Most likely, this is due to the aggregation of the initially formed NZs. To take into account this factor, we call NZs those materials whose nanoscale is confirmed by physical methods for at least one dimension.

The $Zn/Cd/Cu^{bd}$-NZ with the highest R-like activity was chosen for further detailed investigation by SEM coupled with X-ray microanalysis (SEM-XRM). As shown in Fig. 1a–c, NZ has three dimensional flower-like structures with the size of near 1 μm. The XRM images show the characteristic peaks for Cd0, Cu0 and Zn0 (Fig. 1d).

### Catalytic properties of $Zn/Cu/Cd^{bd}$ NZ

**DPPH$^\bullet$ and $ABTS^{\bullet+}$ scavenging activity.** The DPPH$^\bullet$ (1,1-diphenyl-2-picrylhydrazyl radical) and $ABTS^{\bullet+}$ assays have been widely used to determine the free radical-scavenging activity of various plant extracts and chemical compounds. DPPH$^\bullet$ is a stable free radical which, being dissolved in methanol, shows a characteristic absorption peak at 517 nm. The decrease in

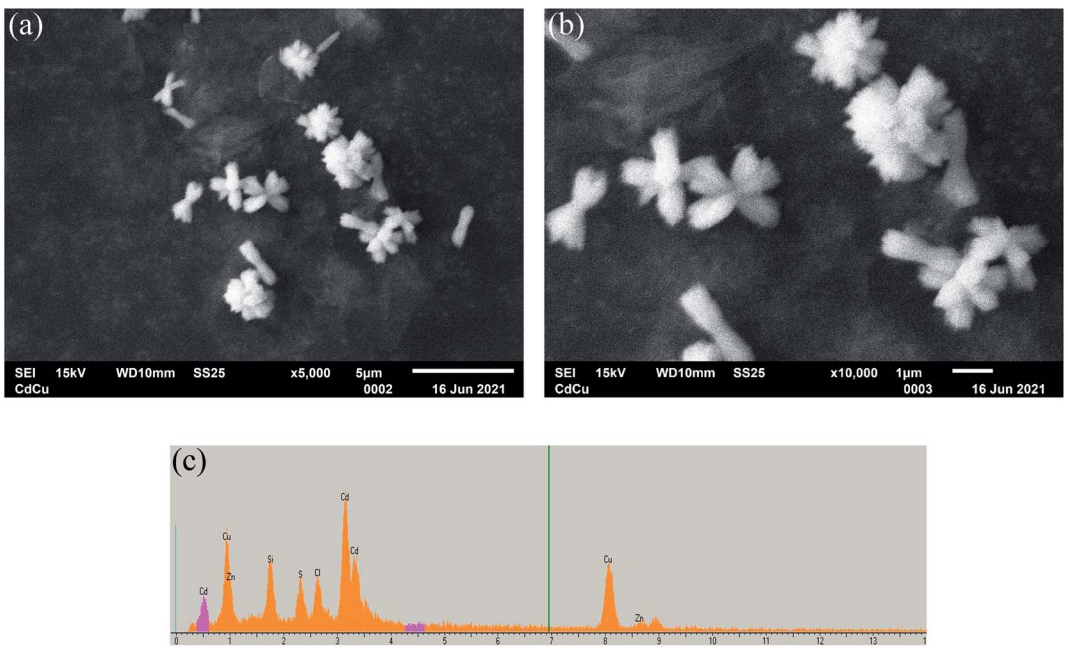


Fig. 1 Characteristics of the $Zn/Cd/Cu^{bd}$ NZ: SEM images for 5000× magnification (scale bar 5 μm) (a) and 10 000× magnification (scale bar 1 μm) (b); X-ray spectral microanalysis (c). The accelerating voltage was 15 kV for all images.

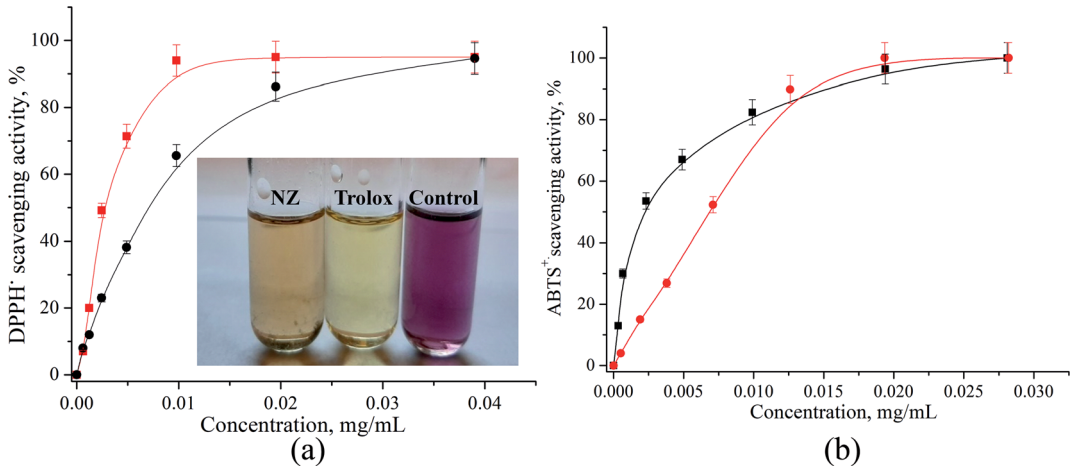


Fig. 2 Dependence of the analytical signal on concentration of Trolox (red) and Zn/Cd/Cu$^{bd}$ NZ (black) in free radical scavenging tests: (a) spectrophotometric DPPH$^{\bullet}$ assay, (b) electrochemical ABTS$^{\bullet+}$ assay.

Table 2 Antioxidant activities ($EC_{50}$) in the samples of Zn/Cd/Cu$^{bd}$ NZ, food products and Trolox determined *via* two methods

| | $EC_{50}$ (μg mL$^{-1}$), that estimated with using | |
|---|---|---|
| Species | DPPH$^{\bullet}$ | ABTS$^{\bullet+}$ |
| Zn/Cd/Cu$^{bd}$ NZ | 6.8 ± 0.2 | 6.9 ± 0.3 |
| Trolox | 2.7 ± 0.1 | 2.9 ± 0.2 |
| Red wine, dry | 2.9 ± 2.0 | ND[a] |
| Bilberry | 9.7 ± 0.1 | 10.5 ± 0.2 |
| Cognac | 12 ± 0.3 | ND |
| Yogurt with chokeberry | 13 ± 1.0 | ND |
| Garnet | 18 ± 2.5 | 19.3 ± 3.0 |
| Tomatoes | 26 ± 0.4 | ND |
| Lemon | 49 ± 0.3 | ND |
| Milk | 582 ± 3.4 | ND |

[a] Not done.

optical absorbance of DPPH$^{\bullet}$ radicals is caused by antioxidants due to the reaction between antioxidant molecules and the radical, which results in the scavenging of the radical by hydrogen donation. Antioxidant capacity estimated by the DPPH$^{\bullet}$ in solution was compared by the electrochemical method with ABTS$^{\bullet+}$. The monitored electrochemical signal was the cathodic current produced from reduction of the ABTS$^{\bullet+}$ radical at the applied potential −0.10 V *vs.* Ag/AgCl on the GE working electrode. The responses were obtained as a current–time plot. The peak currents from antioxidant samples were calibrated with Trolox as a standard in the concentration range of 0–0.03 mg mL$^{-1}$.

As demonstrated in Fig. 2a and b, Zn/Cd/Cu$^{bd}$ NZ shows appreciable DPPH$^{\bullet}$ and ABTS$^{\bullet+}$ free radical scavenging activities at the selected range of concentrations. It was observed that the DPPH$^{\bullet}$ and ABTS$^{\bullet+}$ radical scavenging effect increases with the increase of the concentration of Zn/Cd/Cu$^{bd}$ NZ. The results of the electrochemical ABTS$^{\bullet+}$ method reported in Trolox equivalent units were in good agreement with a classic spectrophotometric DPPH$^{\bullet}$ method. We have tested the samples of some plant foods (berries, vegetables, fruits) and beverages on their antioxidant capacity in comparison with Trolox as a standard. These activities were expressed as $EC_{50}$ values and presented in Table 2.

The $EC_{50}$ values calculated from DPPH$^{\bullet}$ and ABTS$^{\bullet+}$ assays ranged between 9.7–49 mg mL$^{-1}$ for food products and 2.9–12 mg mL$^{-1}$ – for beverages. The values of antioxidant activities determined by two different methods are very similar. It should be noted that the lower $EC_{50}$ value indicates a higher antioxidant activity for the product. The antioxidant activity values determined by these two different assays (Table 2) revealed that among food products and beverages, the Zn/Cd/Cu$^{bd}$ NZ has a stronger antioxidant power when compared to garnet, lemon or milk and a lower power when compared to red wine and the standard Trolox. The obtained $EC_{50}$ data of food products are in good correlation with the data described in literature.[50]

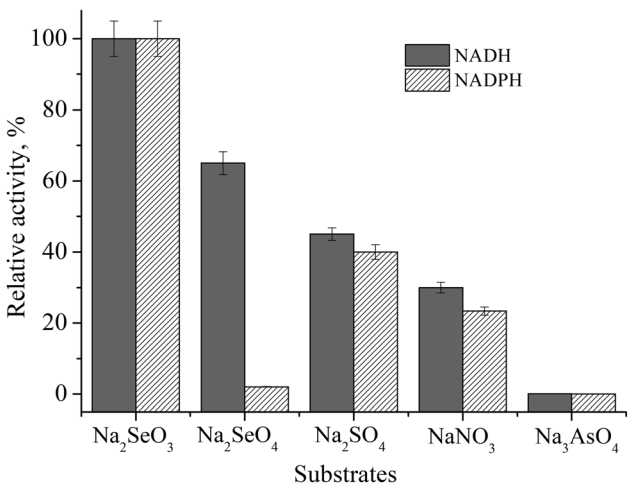


Fig. 3 Substrate and co-factor specificity of Zn/Cd/Cu$^{bd}$ NZ in acetate buffer, pH 4.5. Substrates (1 mM): $Na_2SeO_3$, $Na_2SeO_4$, $Na_2SO_4$ $NaNO_3$ and $Na_3AsO_4$; cofactors (0.13 mM): NADH and NADPH.

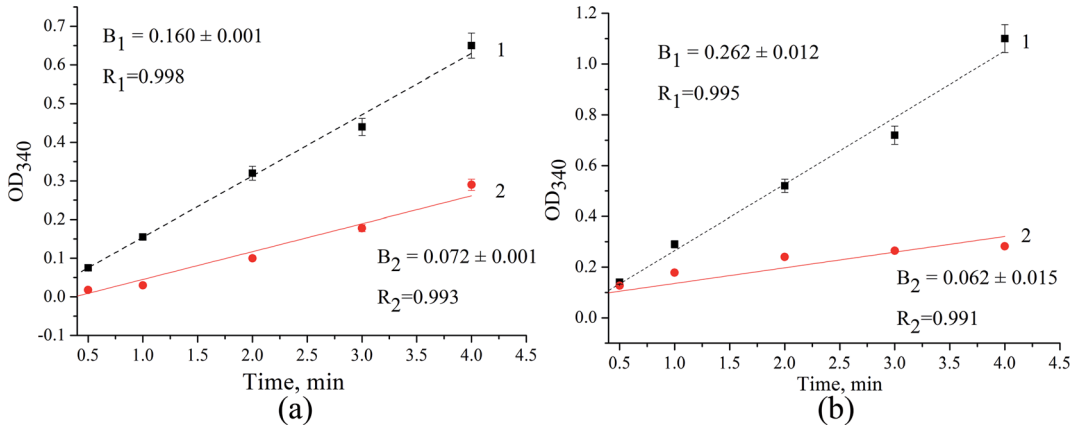


Fig. 4 The kinetic curves for selenite reduction in the mixture of $Na_2SeO_3$, NADH, ABTS (a) or DPPH (b) in acetate buffer, pH 4.5 in the presence (line 1) and in the absence of Zn/Cd/$Cu^{bd}$ NZ (line 2).

**Substrate specificity of pseudo-reductase in solution.** The synthesized NZ was tested on its R-like activity toward different substrates using nicotinamide adenine dinucleotide reduced (NADH) or nicotinamide adenine dinucleotide phosphate reduced (NADPH) as cofactors of reductases (Fig. 3). This NZ possess a high R-like activity in the presence of NADH toward different substrates: $Na_2SeO_3$ (100%), $Na_2SeO_4$ (65%), $Na_2SO_4$ (35%), $NaNO_3$ (45%) and $Na_3AsO_4$ (less than 1%), whereas in the presence of NADPH it shows a lower R-like activity toward the same substrates: $Na_2SeO_3$ (100%), $Na_2SeO_4$ (2%), $Na_2SO_4$ (40%), $NaNO_3$ (23%) and $Na_3AsO_4$ (less than 1%).

We have found that the formation of elemental selenium ($Se^0$) in the presence of cofactors (NADH or NADPH), mediators of electron transfer (ABTS or DPPH), and $Na_2SeO_3$ as a substrate takes place even without the addition of NZ (Fig. 4a and b, lines 2). The addition of Zn/Cd/$Cu^{bd}$ NZ activates this process (Fig. 4a and b, lines 1).

The efficiency factor ($F$) of selenite reduction/$Se^0$ formation for NZ was calculated as a relation of slope values ($F = B_1/B_2$) from the correspondent kinetic curves. In the presence of ABTS in reaction mixture (Fig. 4a), $F_{ABTS}$ is 2.2, whereas in the presence of DPPH (Fig. 4b), the value of $F_{DPPH}$ is 1.8 fold higher and achieves 4.2.

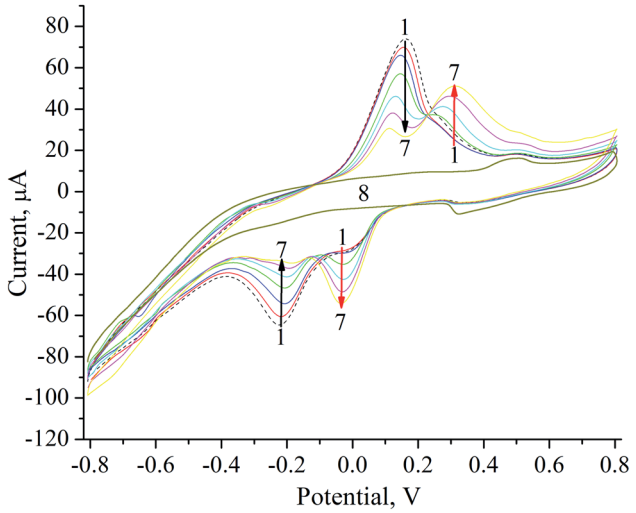


Fig. 5 Cyclic voltammograms of NZ/GE (1–7) and unmodified GE (8) in acetate buffer, pH 4.5 upon subsequent additions of $Na_2SeO_3$, μM: 0 (1), 8 (2), 16 (3), 32 (4), 64 (5), 150 (6), 300 (7, 8).

## Construction, evaluation and application of amperometric sensor for selenite determination

**Optimization of selenium sensing.** The electrochemical characteristics of Zn/Cd/$Cu^{bd}$-NZ, immobilized on the surface of a graphite electrode (NZ/GE), were studied (Fig. 5). The comparison of cyclic voltammograms revealed a cathodic reduction peak at the potential of −50 mV. This peak is possibly related with the $Se^0$ formation on the electrode surface during the reduction of the added $Na_2SeO_3$.[51,52]

Formation of elemental selenium ($Se^0$) on the surface of NZ/GE was visually observed and proved by the SEM and X-ray microanalysis (Fig. 6). According to SEM images, $Se^0$ is generated as agglomerates with the sizes varying from 5 to 50 μm (Fig. 6a, d, e and g). $Se^0$ formation has been proved by X-ray microanalysis, which showed emission peaks at 1.37, 11.22, and 12.49 keV (Fig. 6b, c, f, h and l) corresponding to the $SeL_\alpha$, $SeK_\alpha$, and $SeK_\beta$ transitions, respectively.

The general scheme of the reactions running on the electrode surface can be described as follows: $SeO_3^{2-}$ ions diffuse to the Zn/Cd/$Cu^{bd}$-modified GE and are reduced to $Se^0$ in the presence of NADH and $ABTS^{\bullet+}$. In turn, the NADH cofactor is oxidized to $NAD^+$ and the $ABTS^{\bullet+}$ radical cation is reduced to ABTS releasing 4 electrons and providing a reversible process (Fig. 7). It was shown that the peaks at +300 mV and −50 mV are corresponded to the oxidation of $Se^0$ to $SeO_3^{2-}$ and to the reduction of $SeO_3^{2-}$ to $Se^0$, respectively. The obtained oxidation/reduction peaks for the pair of $SeO_3^{2-}/Se^0$ are in good agreement with the literature data.[53] It should be noted that the reduction $SeO_3^{2-}$ to $Se^0$ on the Zn/Cd/$Cu^{bd}$/GE does not take place in the absence of NADH or ABTS (the data not shown).

**Analytical characteristics of sensor.** A chronamperometric analysis of $Na_2SeO_3$ at −50 mV is provided in Fig. 8. It is worth mentioning that no signals on $Na_2SeO_3$ at the unmodified electrode in the presence of NADH and ABTS were detected at

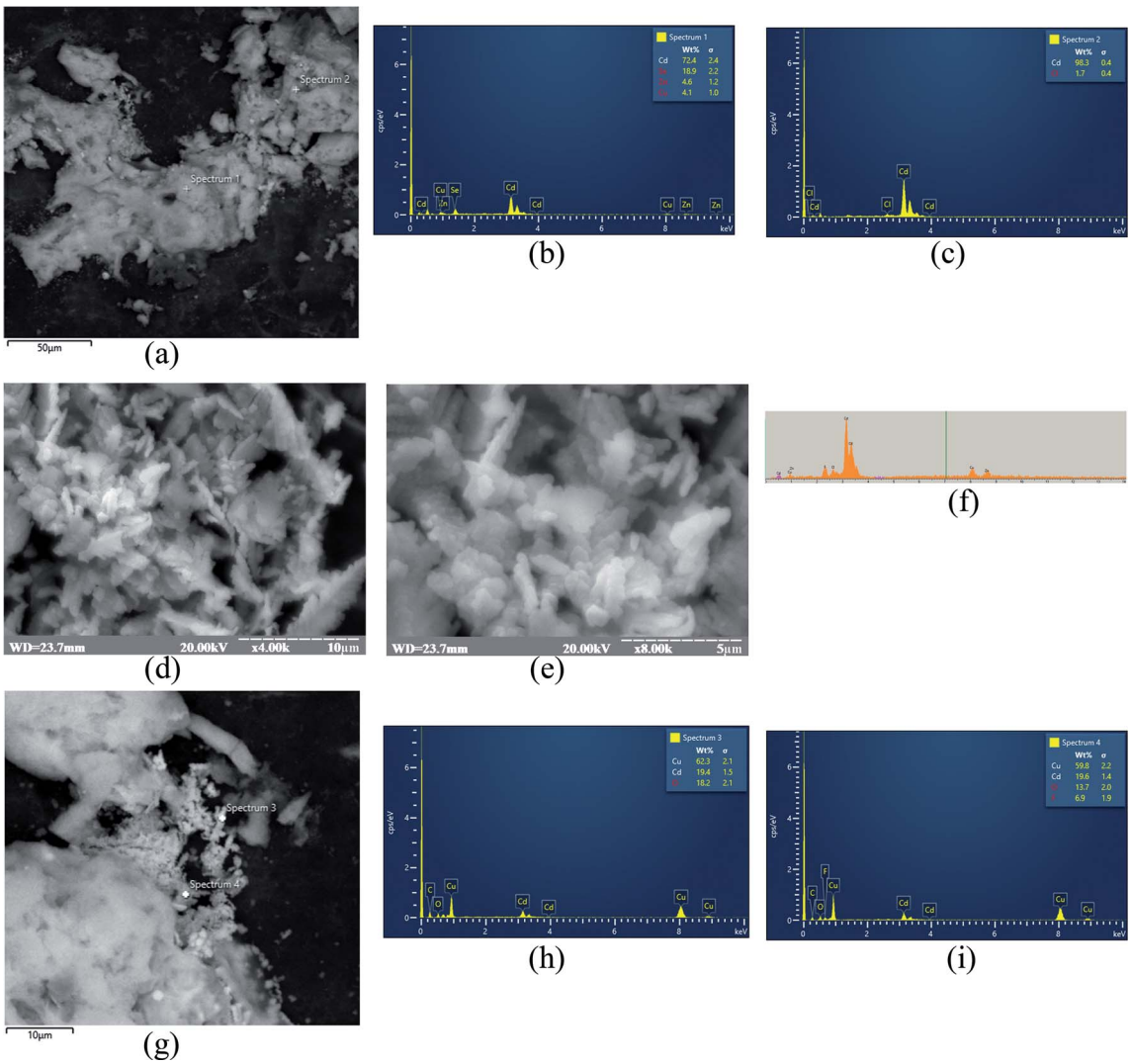


Fig. 6 Characteristics of Zn/Cd/Cu$^{bd}$ NZ: SEM images for scale bar 50 μm (a), 10 μm (d and g), 5 μm (e) for 4000× (a, d and g) and 8000× (e) magnification; X-ray spectral microanalysis (b, c, f, h and i). The accelerating voltage was 20 kV for all images.

these conditions (see Fig. 5). The main characteristics of the $SeO_3^{2-}$-chemosensor were estimated (see Fig. 8b–d). As shown the maximal current of a chronoamperometric response of Zn/Cd/Cu$^{bd}$/GE on the analyte is 142.3 ± 3.0 μA ($d$ = 3.05 mm, $S$ = 7.07 mm$^2$) with a constant of semi-saturation ($K_M^{app}$) 1.25 ± 0.05 mM for $Na_2SeO_3$. The specific sensitivity for Zn/Cd/Cu$^{bd}$/GE is 1700 A M$^{-1}$ m$^{-2}$.

**Assay of selenite in real water samples.** Se is one of the micronutrients for living organisms, although it is one of major concerns due to a narrow range between deficit and toxicity levels.[33,34] In natural environments, including ground water, Se mainly exists as anionic forms of selenate ($SeO_4^{2-}$) and selenite ($SeO_3^{2-}$). The presence of toxic selenite in drinking water at high concentrations is undesirable.[54,55] The number of microorganisms can metabolize selenite from ground water by biological reduction forming solid low toxic nanoparticles of elemental selenium (SeNPs).[33–36]

The levels of Se in groundwater and surface water usually range from 0.06 μg L$^{-1}$ to about 400 μg L$^{-1}$, but in some areas, the Se concentration may to achieve 6000 μg L$^{-1}$.[54] Levels of Se in tap water samples from public water supplies around the world are usually much less than 10 μg L$^{-1}$, although they may exceed 50 μg L$^{-1}$.

The developed selenite specific sensor was tested on the model solution of water (after adding a known concentration of sodium selenite) as well as on the real sample of "Morshynska Antioxiwater, Se + Cr + Zn" mineral water. The results

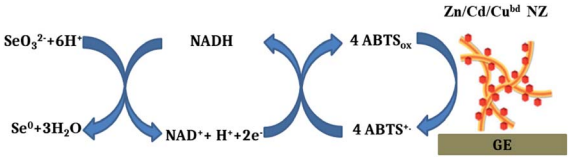


Fig. 7 Hypothetical principal scheme of functionality of the Zn/Cd/Cu$^{bd}$-based amperometric sensor for selenite.

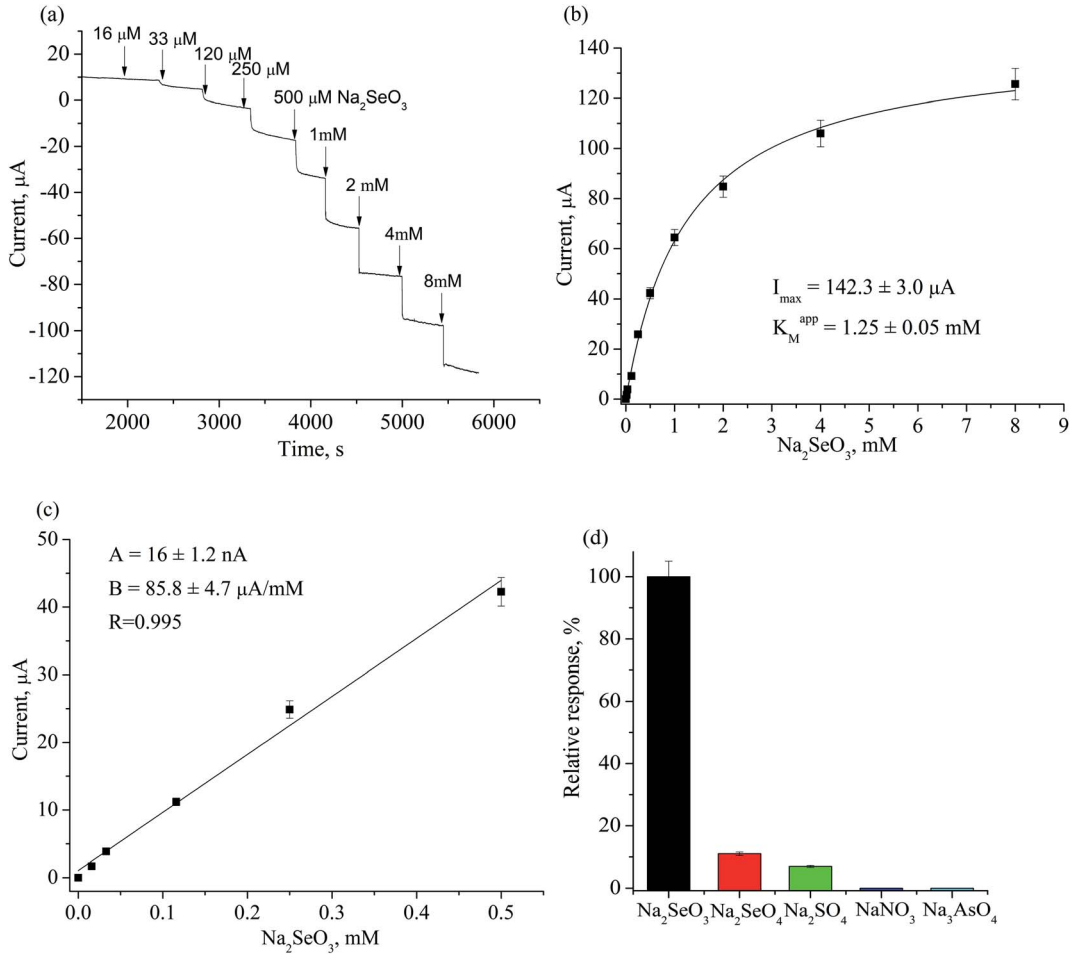


Fig. 8 Characteristics of Zn/Cd/Cu$^{bd}$/GE in 50 mM acetate buffer, pH 4.5: (a) chronamperometric current response upon subsequent additions of $Na_2SeO_3$; (b) dependence of amperometric signal on selenite concentration; (c) calibration graph for $Na_2SeO_3$ determination in linear range; (d) selectivity test for Zn/Cd/Cu$^{bd}$/GE towards different analytes (1 mM) in the presense of 0.13 mM NADH and 1 mM ABTS.

Table 3 Analysis of selenite in model and real samples

| | Concentration of selenite, mg $L^{-1}$ | |
|---|---|---|
| Sample | Sensor analysis | Added to the model sample or declared by producer |
| Model solution, CV,[a] % | 46 ± 2.4, 5.4 | 43.3 ± 1.6 (added) |
| Mineral water "Morshynska", CV, % | 0.0605 ± 0.003, 7.3 | 0.092[b] (declared) |

[a] CV – coefficient of variation. Values are expressed as mean ± SD. [b] Total Se in the form of $SeO_3^{2-}$ and $Se^{2-}$.

of estimation of $SeO_3^{2-}$ in tested waters are presented in Table 3.

The reproducibility of the proposed analytical method is satisfactory: the coefficients of variation (CV) are less than 10%. It is worthwhile mentioning that the detected selenite contents in the water were close to those found by other authors (0.06–400 μg $L^{-1}$).[54] These results indicate that the developed Zn/Cd/Cu$^{bd}$ NZ-based amperometric sensor can be utilized for a fast and simple assay of selenite in water.

# Experimental

## Materials and methods/reagents

Cerium(III) chloride, ascorbic acid, cadmium(II) chloride, chloroplatinic acid, copper(II) sulfate, zinc(II) sulfate, palladium chloride, sodium borohydride, 2,2′-azinobis-(3-ethylbenzothiazoline-6-sulfonic acid) diammonium salt (ABTS), 2,2-diphenyl-1-picrylhydrazyl (DPPH), cetrimonium bromide (CTAB), nicotinamide adenine dinucleotide reduced (NADH), nicotinamide adenine dinucleotide phosphate reduced

(NADPH), Nafion (5% solution in 90% low-chain aliphatic alcohols), potassium persulfate and all other reagents and solvents used in this work were purchased from Sigma-Aldrich (Steinheim, Germany). The antioxidant standard was Trolox from Merck KGaA (Darmstadt, Germany). All reagents were of analytical grade and were used without further purification. All solutions were prepared using ultra-pure water obtained with the Milli-Q® IQ 7000 Water Purification system (Merck KGaA, Darmstadt, Germany).

### Synthetic procedures

**Synthesis of nanozymes by chemical reduction.** NZs were synthesized by the reduction of metal ions from appropriate salts using ascorbic acid. The conditions of NZs synthesis are presented in Table 4. NZs were collected by centrifugation under 16 000*g* for 40 min (Hettich Micro-22R centrifuge), washed twice with water, and precipitated by centrifugation. Pellets were suspended in 1.0 mL water and stored until use at +4 °C.

The synthesis of core–shell NZs on stainless steel substrate was performed by chemical bath deposition method (bd) similar as reported earlier,[56,57] with some modifications. They include preparation of an aqueous bath containing 0.1 M solution of salt, namely, cadmium(II) chloride, palladium(II) chloride or cerium(II) chloride with the addition of aqueous $NH_3$ solution (28%) under constant stirring at room temperature with resultant pH ~ 12. Well cleaned Zn plate substrate was placed in reaction bath at room temperature for 20 h resulting in the direct growth of metallic nanowires on Zn substrate.

For the formation of core–shell Zn/Cd/Cu$^{bd}$ NZs, the previously synthesized Cd/Zn thin film was vertically dipped into beaker containing 0.01 M copper sulphate solution making an angle of 45° with the wall of beaker. The reaction bath maintained at room temperature for 3 days resulting in the conversion of gray color cadmium film into brown color. The resulting Zn/Cd/Cu$^{bd}$ NZs were washed several times with water, dried in air atmosphere and used for further characterization.

**Morphological analysis of megazymes by scanning electron microscopy (SEM).** Morphological analyses of the reductase-like (R-like) NZs were performed using a microanalyzer Hitachi S-3400N SEM. The Energy Dispersive X-ray Spectroscopy component is implemented with an EDAX EDS. The samples in different dilutions (2 μL) were dropped onto the surface of a silicon wafer and were dried at room temperature. The distance from the last lens of the microscope to the sample (WD) was 10 mm. The accelerator voltage was in the range of 20 to 40 eV.

Table 4 Methods of chemical synthesis of NZs

| No. | NZ | Reaction mixture and conditions |
|---|---|---|
| 1 | Cd/Cu | 5 mL 100 mM $CdCl_2$ + 10 mL 12.5 mM CTAB, vigorous stirring for 5 min at 20 °C followed by adding 0.2 mL 100 mM ascorbic acid and heating at 100 °C during 10 min; +5 mL 100 mM $CuSO_4$ followed by adding 0.2 mL 100 mM ascorbic acid, heating at 100 °C and stirring for 15 min at 20 °C |
| 2 | Ce/Pd | 5 mL 100 mM $CeCl_3$ + 10 mL 12.5 mM CTAB, vigorous stirring for 5 min at 20 °C followed by adding 0.2 mL 100 mM ascorbic acid and heating at 100 °C during 10 min; +5 mL 100 mM $PdCl_3$ followed by adding 0.2 mL 100 mM ascorbic acid, heating at 100 °C and stirring for 15 min at 20 °C |
| 3 | Cu/Pt | 5 mL 100 mM $H_2PtCl_6$ + 10 mL 12.5 mM CTAB, vigorous stirring for 5 min at 20 °C followed by adding 0.2 mL 100 mM ascorbic acid and heating at 100 °C during 10 min; +5 mL 100 mM $CuSO_4$ followed by adding 0.2 mL 100 mM ascorbic acid, heating at 100 °C and stirring for 15 min at 20 °C |
| 4 | Ce | 5 mL 100 mM $CeCl_3$ + 10 mL 12.5 mM CTAB, vigorous stirring for 5 min at 20 °C followed by adding 0.2 mL 100 mM ascorbic acid and heating at 100 °C during 10 min |
| 5 | Cd/Pd | 5 mL 100 mM $PdCl_3$ + 10 mL 12.5 mM CTAB, vigorous stirring for 5 min at 20 °C followed by adding 0.2 mL 100 mM ascorbic acid and heating at 100 °C during 10 min; + 5 mL 100 mM $CdCl_2$ followed by adding 0.2 mL 100 mM ascorbic acid, heating at 100 °C and stirring for 15 min at 20 °C |

### Determination of pseudo-enzymatic activities of nanomaterials in solution

**ABTS-based method.** Screening of the synthesized NZs on their R-like activities was done spectrophotometrically using ABTS cation radical ($ABTS^{\bullet+}$) as a chromogenic substrate. To obtain $ABTS^{\bullet+}$, 7 mM solution of ABTS was mixed with equal volume of 2.4 mM potassium persulfate solution, and the mixture was incubated during 12 h at room temperature in the dark. The resultant 3.5 mM $ABTS^{\bullet+}$ solution was diluted with methanol up to the optical density of approximately 0.70 at 734 nm.

The procedure of the assay was the following: 10 μL aqueous suspension of NZ was incubated in a glass tube with 1 mL of the chromogenic substrate ($ABTS^{\bullet+}$ solution). Addition of NZ to the substrate stimulated the discoloration from dark blue to colorless over time, indicating an pseudo-enzymatic reaction. The reaction was monitored kinetically during 5 min. The analytical results were statistically processed using the OriginPro 8.5 software.

The specific R-like activity was expressed in μmol $min^{-1}$ $mg^{-1}$ of NZ and calculated using the following formula:

$$\text{Specific capacity, U mg}^{-1} = \frac{\Delta D/\text{min} \times V_t \times N}{17 \times V_{AE} \times c}, \quad (1)$$

where $\Delta D_{734}$/min – drop in optical density for 1 minute; $V_t$ – the total volume of the reaction mixture in the cuvette, mL; 17 – millimolar extinction coefficient of the $ABTS^{\bullet+}$, $mM^{-1}$ $cm^{-1}$; $V_{AE}$ – aliquot of AE added, mL; $c$ – mass concentration of NZ in added solution, determined by gravimetric method, mg $mL^{-1}$; $N$ – dilution of NZ before adding to the reaction mixture; 1 unit (U) of activity corresponds to 1 μmole $ABTS^{\bullet+}$ reduced during 1 min under indicated conditions.

**DPPH-based method.** In solution the antioxidant properties were determined *via* the DPPH$^{\bullet}$-based free radical scavenging test according to modified method of Brand-Williams *et al.*[58] 0.04 mL Zn/Cd/Cu$^{bd}$ solution in different concentrations (0.31, 0.62, 1.25, 2.5 and 5 mg mL$^{-1}$) was mixed with 1.2 mL freshly prepared DPPH$^{\bullet}$ (1 mM in methanol) solution and vortexed thoroughly. Then the solution was incubated for 30 min at room temperature in the dark. The absorbance was recorded at 517 nm using UV-Vis spectrophotometer (Shimadzu, U-1860). When an antioxidant scavenges the free radicals by hydrogen donation, the colors in the DPPH$^{\bullet}$ assay solution become lighter. DPPH (all the reagent except the sample) was used as a control and methanol was used as a blank solution. The free radical scavenging activity was expressed as the percentage of inhibition which was determined using the following formula (2):

$$\text{Percentage scavenging} = \frac{Z_p - Z_q}{Z_p} \times 100\%, \quad (2)$$

where $Z_p$ is an optical density of control (all the reagent except the test sample), while $Z_q$ is an optical density of the tested sample.

Electrochemical assay of the free radical scavenging activity was done using the ABTS$^{\bullet+}$ based method.[59]

**Apparatus, measurements, and statistical analysis.** The amperometric sensors were evaluated using constant-potential amperometry in a three-electrode configuration with an Ag/AgCl/KCl (3 M) reference electrode, a Pt-wire counter electrode and a graphite working electrode. Graphite rods (type RW001, 3.05 mm diameter) from Ringsdorff Werke (Bonn, Germany) were sealed in glass tubes using epoxy glue to form disk electrodes. Before sensor preparation, the GE was polished with emery paper and a polishing cloth using decreasing particle sizes of alumina paste (Leco, Germany). The polished electrodes were rinsed with water in an ultrasonic bath.

Amperometric measurements were carried out using a CHI 1200A potentiostat (IJ Cambria Scientific, Burry Port, UK) connected to a personal computer and performed in a batch mode under continuous stirring in an electrochemical cell with a 20 mL volume at 25 °C.

All experiments were carried out in triplicate trials. Analytical characteristics of the electrodes were statistically processed using the OriginPro 2021 software. The error bars represent the standard error derived from three independent measurements. Calculation of the apparent Michaelis–Menten constants ($K_M^{app}$) was performed automatically by this program according to the Lineweaver–Burk equation.

**Immobilization of NZs onto electrodes, testing their electrochemical and R-like activity.** For construction of the NZs-based electrode, 5 μL NZ suspension (1 mg mL$^{-1}$) was dropped onto the surfaces of GEs. After drying for 10 min at room temperature, the layer of NPs on the electrodes was covered with 5 μL Nafion solution. The electrodes were washed with corresponding buffer solutions before and after each measurement.

The electrochemical properties of the synthesized NZs were studied by cyclic voltammetry (CV) on the GEs in the range from −800 to +800 mV with the scan rate of 50 mV min$^{-1}$; the profiles of amperometric signals in increasing concentrations of $Na_2SeO_3$ were compared.

The monitored signal was the cathodic current produced from reduction of the ABTS$^{\bullet+}$ radical at the applied potential −0.10 V *vs.* Ag/AgCl on the GE working electrode. The responses were obtained as the current–time plot. The peak currents from antioxidant samples were calibrated using Trolox as a standard in concentration range 0–28 μg mL$^{-1}$.

**Selenite ions assay in real samples.** The constructed Zn/Cd/Cu$^{bd}$ NZ-based amperometric sensor for selenite determination was tested on the real and model samples. Commercial mineral antioxiwater «Morshynska» (Morshyn, Ukraine), containing Se + Cr + Zn, was analysed using a standard addition test (SAT). A model sample is a fresh-prepared $Na_2SeO_3$ solution of exact concentration in distilled water. Each assay was performed for two dilutions of the sample and repeated 3 times. The analytical results were statistically processed using the OriginPro 2021 software.

## Conclusions

In the current research, a number of nano- and microzymes based on transition and noble metals were synthesized by the reduction and chemical bath deposition methods. The antioxidant and radical-scavenging properties of the synthesized Zn/Cd/Cu$^{bd}$ NZ were studied by its ability to reduce the DPPH$^{\bullet}$ or ABTS$^{\bullet+}$ radicals in solution. The structure, size, morphology, composition, catalytic properties, and electrochemical activities of the chosen Zn/Cd/Cu$^{bd}$ NZ in solution and in immobilized form on the electrode were characterized.

The novelty of the work is the following: (1) obtaining for the first time the nanozymes with a high reductase activity; (2) the discovery of the nanozyme with selenite-specific reducing activity; (3) the construction of selenite-selective chemosensor based on metal hybrid nanocomposite. Being sensitive, valid, low-cost, highly selective, the proposed nanozyme-based chemosensor would be promising in different fields of fundamental and practical science, including environmental chemistry, plant and animal biochemistry, nutrition, and medicine.

Because of a high antioxidant activity of the synthesized nanozymes, we plan to study in future the influence of the nanozymes *in vivo* on eucaryotic cells to test possible consequences of nanozymes' uptake on cell viability and redox-activity of the modified living cells.

## Funding

This research was partially supported by the National Research Foundation of Ukraine (projects no. 2020.02/0100 "Development of new nanozymes as catalytic elements for enzymatic kits and chemo/biosensors" and 2021.01/0010 "Development of an enzymatic kit and portable biosensors for express-analysis of creatinine, a marker of acute functional disorders of the kidneys"), National Academy of Sciences of Ukraine (The program "Smart sensor devices of a new generation based on modern materials and technologies"; grant "New dual casein

kinase 2 inhibitors and histone deacetylase for targeted tumor chemotherapy" for research laboratories/groups of young scientists in priority areas of science and technology in 2021–2022), and Ministry of Education and Science of Ukraine (projects no. 0120U103398, 0121U109539 and 0121U109543).

## Author contributions

Nataliya Stasyuk and Galina Gayda: investigation, validation, writing – original draft, visualization. Taras Kavetskyy: methodology, formal analysis, visualization. Mykhailo Gonchar: conceptualization, supervision, writing – review & editing, project administration, funding acquisition, resources.

## Conflicts of interest

There are no conflicts to declare.

## Acknowledgements

The authors thank Dr I. Mat'ko (Institute of Physics, Slovak Academy of Sciences, Bratislava, Slovakia) and R. Serkiz (Institute of Cell Biology NAS of Ukraine, Lviv, Ukraine) for their help with SEM-XRM experiments.

## References

1 H. Wei and E. Wang, *Chem. Soc. Rev.*, 2013, **42**, 6060–6093.
2 R. Tian, J. Xu, Q. Luo, C. Hou and J. Liu, *Front. Chem.*, 2021, **8**, 1–21, DOI: 10.3389/fchem.2020.00831.
3 J. Wu, X. Wang, Q. Wang, Z. Lou, S. Li, Y. Zhu, L. Qin and H. Wei, *Chem. Soc. Rev.*, 2019, **48**, 1004–1076.
4 N. Stasyuk, O. Smutok, O. Demkiv, T. Prokopiv, G. Gayda, M. Nisnevitch and M. Gonchar, *Sensors*, 2020, **20**, 4509–4550.
5 N. Alizadeh and A. Salimi, *J. Nanobiotechnol.*, 2021, **19**(1), DOI: 10.1186/s12951-021-00771-1.
6 Y. Huang, J. Ren and X. Qu, *Chem. Rev.*, 2019, **119**, 4357–4412.
7 A. A. Nayl, A. I. Abd-Elhamid, A. Y. El-Moghazy, M. Hussin, M. A. Abu-Saied, A. A. El-Shanshory and H. M. A. Soliman, *Trends Environ. Anal. Chem.*, 2020, **26**, e00087, DOI: 10.1016/j.teac.2020.e00087.
8 W. Wang and S. Gunasekaran, *TrAC, Trends Anal. Chem.*, 2020, 115841, DOI: 10.1016/j.trac.2020.115841.
9 N. E. Castillo, E. M. Melchor-Martínez, J. S. Ochoa Sierra, N. M. Ramírez-Torres, J. E. Sosa-Hernández, H. M. N. Iqbal and R. Parra-Saldívar, *Int. J. Biol. Macromol.*, 2021, **179**, 80–89.
10 R. Mahmudunnabi, F. Z. Farhana, N. Kashaninejad, S. H. Firoz, Y. B. Shim and M. J. A. Shiddiky, *Analyst*, 2020, **145**, 4398–4420, DOI: 10.1039/d0an00558d.
11 M. Kumawat, A. Umapathi, E. Lichtfouse and H. K. Daima, *Environ. Chem. Lett.*, 2021, **19**(6), 3951–3957.
12 S. Khan, M. Sharifi, S. H. Bloukh, Z. Edis, R. Siddique and M. Falahati, *Talanta*, 2021, **224**, 121805, DOI: 10.1016/j.talanta.2020.121805.
13 L. Gao, J. Zhuang, L. Nie, J. Zhang, Y. Zhang, N. Gu, T. Wang, J. Feng, D. Yang, S. Perrett and X. Yan, *Nat. Nanotechnol.*, 2007, **2**, 577–583.
14 F. Attar, M. G. Shahpar, B. Rasti, M. Sharifi, A. A. Saboury, S. M. Rezayat and M. Falahati, *J. Mol. Liq.*, 2019, **278**, 130–144.
15 B. Neumann and U. Wollenberger, *Sensors*, 2020, **20**, 3692, DOI: 10.3390/s20133692.
16 R. Fu, J. Zhou, Y. Wang, Y. Liu, H. Liu, Q. Yang, Q. Zhao, B. Jiao and Y. He, *ACS Appl. Bio Mater.*, 2021, **4**(4), 3539–3546.
17 H. Zhao, R. Zhang, X. Yan and K. Fan, *J. Mater. Chem. B*, 2021, **9**, 6939–6957.
18 F. Mancin, L. J. Prins, P. Pengo, L. Pasquato, P. Tecilla and P. Scrimin, *Molecules*, 2016, **21**(8), 1014, DOI: 10.3390/molecules21081014.
19 J. Chen, Q. Ma, M. Li, W. Wu, L. Huang, L. Liu, Y. Fang and S. Dong, *Nanoscale*, 2020, **12**, 23578–23585.
20 S. Biswas and A. Pal, *Mater. Today Commun.*, 2021, **28**, 102588.
21 R. D. Neal, R. A. Hughes, P. Sapkota, S. Ptasinska and S. Neretina, *ACS Catal.*, 2020, **10**(17), 10040–10045.
22 L. Lu, S. Zou and B. Fang, *ACS Catal.*, 2021, **11**(10), 6020–6058.
23 D. Besold, S. Risse, Y. Lu, J. Dzubiella and M. Ballauff, *Ind. Eng. Chem. Res.*, 2021, **60**(10), 3922–3935.
24 A. A. Nafiey, A. Addad, B. Sieber, G. Chastanet, A. Barras, S. Szunerits and R. Boukherroub, *Chem. Eng. J.*, 2017, **322**, 375–384.
25 R. Acharya, A. Lenka and K. Parida, *J. Mol. Liq.*, 2021, **337**, 116487.
26 H. Luck, in *Method of Enzymatic Analysis*, ed. H. U. Bergmeyer, Academic Press, New York and London, 1st edn, 1965, pp. 885–894.
27 F. Hollmann, D. J. Opperman and C. E. Paul, *Angew. Chem., Int. Ed. Engl.*, 2021, **60**(11), 5644–5665.
28 D. R. Lovley, *Annu. Rev. Microbiol.*, 1993, **47**, 263–290.
29 https://www.creative-biolabs.com/metalloreductase-family.html.
30 N. Butler and A. M. Kunjapur, *J. Biotechnol.*, 2020, **307**, 1–14.
31 H. Stolterfoht, D. Schwendenwein, C. W. Sensen, F. Rudroff and M. Winkler, *J. Biotechnol.*, 2017, **257**, 222–232.
32 L. Li, B. Zhang, L. Li and A. G. L. Borthwick, *J. Hazard. Mater.*, 2022, **422**, 126932.
33 E. P. Painter, *Chem. Rev.*, 1941, **28**, 179–213.
34 M. M. Stenchuk, L. B. Chaban and M. V. Gonchar, *Biopolym. Cell*, 2006, **22**(1), 3–17.
35 W. J. Hunter, *Curr. Microbiol.*, 2014, **69**(1), 69–74.
36 M. Wells, J. McGarry, M. M. Gaye, P. Basu, R. S. Oremland and J. F. Stolz, *J. Bacteriol.*, 2019, **201**(7), e00614-18.
37 L. J. Yanke, R. D. Bryant and E. J. Laishley, *Anaerobe*, 1995, **1**(1), 61–67.
38 D. F. Ackerley, C. F. Gonzalez, M. Keyhan, R. Blake and A. Matin, *Environ. Microbiol.*, 2004, **6**, 851–860.
39 A. G. O'Neill, B. A. Beaupre, Y. Zheng, D. Liu and G. R. Moran, *Appl. Environ. Microbiol.*, 2020, **86**(22), e01758-20.

40 J. C. Begara-Morales, M. Chaki, R. Valderrama, C. Mata-Pérez, M. N. Padilla-Serrano and J. B. Barroso, in *Plant Life Under Changing Environment*, ed. D. K. Tripathi, *et al.*, Elsevier, Academic Press, 2020, ch. 29, pp. 735–754.
41 D. J. Richardson, R. van Spanning and S. J. Ferguson, in *Biology of the Nitrogen Cycle*, ed. H. Bothe, S. Ferguson and W. E. Newton, Elsevier, Elsevier Science, 1st edn, 2006, ch. 3.
42 M. Guiral, L. Prunetti, C. Aussignargues, A. Ciaccafava, P. Infossi, M. Ilbert, E. Lojou and M.-T. Giudici-Orticoni, in *Advances in Microbial Physiology*, ed. R. K. Poole, Academic Press, New York, 2012, vol. 61, ch. 4, pp. 125–194.
43 Z. Liang, H. Guo, G. Zhou, K. Guo, H. Lei, W. Zhang, H. Zheng, U.-P. Apfel and R. Cao, *Angew. Chem.*, 2021, **60**(15), 8472–8476.
44 A. A. Vernekar and G. Mugesh, *Chem.–Eur. J.*, 2012, **18**, 15122–15132.
45 K. Li, R. Qin, K. Liu, W. Zhou, N. Liu, Y. Zhang, S. Liu, J. Chen, G. Fu and N. Zheng, *ACS Appl. Mater. Interfaces*, 2021, DOI: 10.1021/acsami.1c11548.
46 S. Singh, S. Ghosh, V. K. Pal, M. Munshi, P. Shekar, D. T. Narasimha Murthy, G. Mugesh and A. Singh, *EMBO Mol. Med.*, 2021, **13**(5), e13314, DOI: 10.15252/emmm.202013314.
47 M. V. Irazabal and V. E. Torres, *Cells*, 2020, **9**(6), 1342, DOI: 10.3390/cells9061342.
48 D. Jiang, D. Ni, Z. T. Rosenkrans, P. Huang, X. Yan and W. Cai, *Chem. Soc. Rev.*, 2019, **48**, 3683–3704.
49 D. Bartolini, A. M. Stabile, S. Bastianelli, D. Giustarini, S. Pierucci, C. Busti, C. Vacca, A. Gidari, D. Francisci, R. Castronari, A. Mencacci, M. Di Cristina, R. Focaia, S. Sabbatini, M. Rende, A. Gioiello, G. Cruciani, R. Rossi and F. Galli, *Redox Biol.*, 2021, **45**, 102041.
50 M. Chochevska, E. J. Seniceva, S. K. Veličkovska, G. Naumova-Leția, V. Mirčeski, J. M. F. Rocha and T. Esatbeyoglu, *Microorganisms*, 2021, **9**(9), 1946.
51 Y. Lai, F. Liu, J. Li, Z. Zhang and Y. Liu, *J. Electroanal. Chem.*, 2010, **639**, 187–192.
52 S. Seyedmahmoudbaraghani, S. Yu, J. Lim and N. V. Myung, *Front. Chem.*, 2020, **8**, 785.
53 A. A. Vernekar and G. Mugesh, *Chem.–Eur. J.*, 2012, **18**, 15122–15132.
54 https://www.who.int/water_sanitation_health/dwq/chemicals/selenium.pdf.
55 S. B. Goldhaber, *Regul. Toxicol. Pharmacol.*, 2003, **38**, 232–242.
56 O. Demkiv, N. Stasyuk, R. Serkiz, G. Gayda, M. Nisnevitch and M. Gonchar, *Appl. Sci.*, 2021, **11**, 777, DOI: 10.3390/app11020777.
57 S. Patil, S. Raut, R. Gore and B. Sankapal, *New J. Chem.*, 2015, **39**, 9124–9131.
58 W. Brand-Williams, M. E. Cuvelier and C. Berset, *LWT–Food Sci. Technol.*, 1995, **28**, 25–30.
59 R. Chaisuksant, K. Damwan and A. Poolkasem, *Acta Hortic.*, 2012, **943**, 297–302.